

Sequential Decoding of Convolutional Codes for Synchronization Errors

Anisha Banerjee, Andreas Lenz and Antonia Wachter-Zeh

Institute for Communications Engineering
Technical University of Munich
DE-80333 Munich, Germany

Email: anisha.banerjee@tum.de, andreas.lenz@mytum.de, antonia.wachter-zeh@tum.de

Abstract—In this work, a sequential decoder for convolutional codes over channels that are vulnerable to insertion, deletion, and substitution errors, is described and analyzed. The decoder expands the code trellis by introducing a new channel state variable, called drift state, as proposed by Davey-MacKay. A suitable decoding metric on that trellis for sequential decoding is derived, in a manner that generalizes the original Fano metric. Under low-noise environments, this approach reduces the decoding complexity by a couple orders of magnitude in comparison to Viterbi’s algorithm, albeit at relatively higher frame error rates. An analytical method to determine the computational cutoff rate is also suggested. This analysis is supported with numerical evaluations of frame error rates and computational complexity, which are compared with respect to optimal Viterbi decoding.

I. INTRODUCTION

Most error-control systems usually operate under the assumption of perfect synchronization between transmitter and receiver, while their respective decoders are designed to detect and correct substitution errors alone. However, when this assumption does not hold, as in the case of some networking and data storage channels [1, 2], some transmitted symbols may be lost or random ones may be inserted into the received stream. Such errors are referred to as deletions and insertions.

There exists rich literature dedicated to the study of channels that are susceptible to insertion, deletion and substitution errors, and suitable error-correcting codes to increase transmission reliability under such environments [3–10]. In this work, we are interested in the use of convolutional codes for the purpose of correcting these errors. Prior work in [11, 12] suggested new trellis structures that helped in adapting the conventional Viterbi and MAP decoders to handle insertions and deletions. One drawback of these decoding approaches however, lies in their memory requirements and computational complexity. In particular, the trellis grows rapidly with factors like constraint length of the code, number of information blocks per codeword and maximum allowable insertions and deletions per block. This motivated us to look into an alternative approach, namely *sequential decoding*.

First proposed by Wozencraft [13], sequential decoders constitute a decoding strategy that is suited to convolutional codes with higher constraint lengths. This is primarily owed to the fact that a typical sequential decoder will only examine those codewords that seem likely to have been transmitted, unlike the Viterbi decoder which assesses all possibilities,

This work has been supported by the European Research Council (ERC) under the European Union’s Horizon 2020 research and innovation programme (Grant Agreement No. 801434).

regardless of noise levels. Though this leads to a worse error-correcting performance, the resultant decoding complexity is effectively independent of the encoder’s memory.

The main objective of this work is to tailor the sequential decoding approach for use in channels that experience insertions, deletions as well as substitution errors. This problem was first addressed by Gallager [9], who used Wozencraft’s original algorithm to implement the sequential decoder, and subsequently analyzed its complexity. Mansour and Tewfik [14] also worked on this problem, by adopting a new trellis structure and specifically limiting their focus to the stack algorithm. However, unlike [9, 14], this work formulates a new decoding metric, wherein the likelihood component is computed using the lattice metric [15], and an additional bias term accounts for probability of the predicted message sequence and that of the received bit sequence. Furthermore, we employ the trellis structure proposed in [12] and limit our attention to Fano’s algorithm, which typically performs fewer computations and explores more paths compared to other variants of sequential decoding.

II. PRELIMINARIES

A. Channel model

As in [5, 15], we adopt a finite state machine model for our channel, specified by three parameters P_i , P_d and P_s , which denote the insertion, deletion and substitution probabilities of the channel, respectively. Let $\mathbf{x}_1^M = (x_1, \dots, x_M) \in \{0, 1\}^M$ denote a sequence of bits awaiting transmission. From Fig. 1, we observe that under this construct, for each input bit, one of four events may occur: a random bit is inserted into the received stream with probability P_i and x_i remains in the transmission queue; or the next bit queued for transmission, i.e., x_i , is deleted with probability P_d ; or x_i is received at output end, either erroneously or correctly, with probabilities $P_t P_s$ and $P_t (1 - P_s)$ respectively. Here, $P_t = 1 - P_i - P_d$ simply refers to the transmission probability.

B. Convolutional codes

Before describing the decoding framework, we shortly recapitulate the basics of convolutional codes. These codes constitute a special category of tree codes, that incorporate memory and aim to encode a stream of input bits in a block-wise manner, by means of shift registers. They are typically specified by three parameters: $[c, b, m]$, indicating that for every b input bits received, the encoder generates c output bits, which are a function of the last $b(m+1)$ input bits.

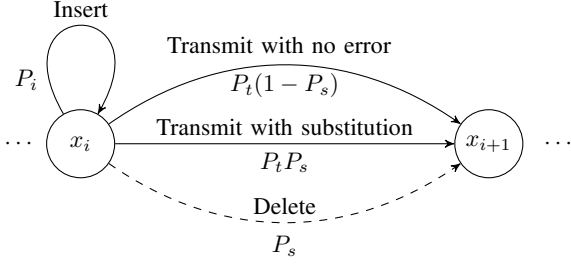


Figure 1. Allowed transitions in the state machine model for the insertion, deletion, and substitution channel [5]

C. Joint code and channel tree structure

As in [12], the vector obtained at the receiving end of the channel is viewed as the output of a hidden Markov model (HMM), where each hidden state is a pair of the encoder state and the drift value. In this context, we define the *drift* [5] as the difference between number of bits received and transmitted. In particular, d_i is used to signify the net drift accumulated after the transmission of i bits. For more details about the drift variable, we refer the reader to [5].

The decoder works on a tree representation of this HMM, such that any path in this tree describes how the encoder state and net drift value could change over time. As a demonstration, Fig. 2 depicts the joint code and channel tree for a $[3, 1, 1]$ convolutional encoder. For any given sequence of HMM states, the concatenation of edge labels along the respective path in the code tree indicates the originally transmitted codeword.

D. Fano's Algorithm

In this work, we limit our focus to a particular variant of sequential decoding, namely Fano's algorithm [16]. It operates on the principle that node metrics along the correct path keep increasing on an average. The algorithm searches for such a path, by tracking metrics of the current, previous and best successor nodes, denoted as μ_c , μ_p and μ_s respectively. A dynamic threshold T is used to check for the aforementioned property. This variable can only be altered by integer multiples of a user-defined step size Δ . Starting from tree root, the decoder works as follows:

- 1) If best successor has metric $\mu_s \geq T$, move forward.
 - If this node has never been visited before, T is tightened such that
$$T \leq \mu_c < T + \Delta. \quad (1)$$
- 2) Else, step back to the immediate predecessor.
 - If other successors with metrics above T exist, the decoder steps forward to it, as in step 1).
 - Else:
 - If $\mu_p < T$, lower T by Δ .
 - Else repeat step 2).

In this manner, all the paths with metrics above or equal to the threshold T are systematically explored.

III. DECODER METRIC

From the preceding discussion, it is evident that a metric for each tree node must be defined to quantify its closeness to the

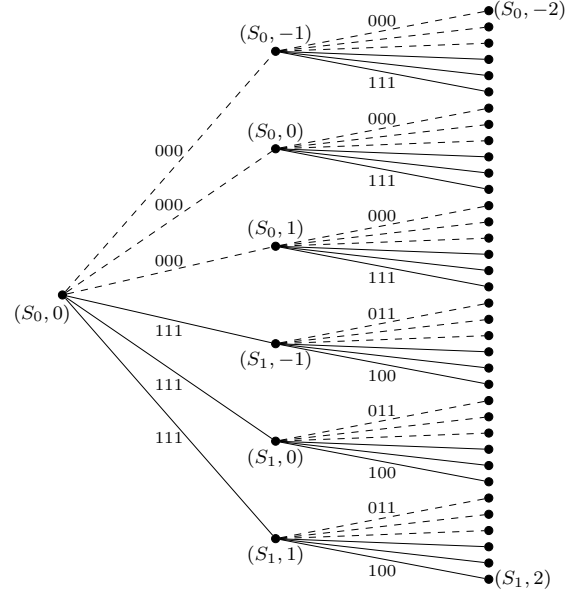


Figure 2. Joint code and channel tree of a $[3, 1, 1]$ convolutional code. Dashed lines correspond to an input of 0 and solid lines to input 1. Each node has two state variables, the convolutional code state and the drift state.

received vector. Specifically, this metric should help minimize the probability of choosing a wrong successor.

Let $\mathbf{y}_1^N = (y_1, \dots, y_N)$ denote a received sequence produced by the transmission of a codeword of L blocks. Now consider a path in the corresponding code tree for a convolutional code with parameters $[c, b]$, from the root to a node at depth t , say \mathbf{v}_t , that corresponds to the sequence of convolutional code states $\mathbf{s}_0^t = (s_0, \dots, s_t)$ and the drift state vector $\mathbf{d}_0^t = (d_0, d_c, \dots, d_{ct})$, where initial drift is $d_0 = 0$. Then, the metric of node \mathbf{v}_t in the tree is given by

$$\begin{aligned} \mu(\mathbf{v}_t) &= \log_2 P(\mathbf{v}_t | \mathbf{y}_1^N) \\ &= \log_2 P(\mathbf{v}_t, \mathbf{y}_1^N) - \log_2 P(\mathbf{y}_1^N) \\ &= \log_2 P(\mathbf{s}_0^t, \mathbf{d}_0^t, \mathbf{y}_1^N) - \log_2 P(\mathbf{y}_1^N). \end{aligned} \quad (2)$$

Hence, the decoder metric of a path is essentially the probability of its predicted codeword and drift changes, given a specific received frame. This definition is in the same spirit as that in [17], wherein Massey proved the optimality of the Fano metric in the context of binary symmetric channels.

Before further simplifying (2), we recognize that the path \mathbf{v}_t only accounts for the first $ct + d_{ct}$ symbols of the received vector. The remaining symbols $\mathbf{y}_{ct+d_{ct}+1}^N$ are assumed to have been produced by a tailing message sequence that guides the convolutional encoder through the states $\tilde{\mathbf{s}}_{t+1}^L = (s_{t+1}, \dots, s_L)$. Additionally assuming that $\mathbf{y}_{ct+d_{ct}+1}^N$ is unaffected by bits transmitted prior to it, we may write

$$\begin{aligned} P(\mathbf{v}_t, \tilde{\mathbf{s}}_{t+1}^L, \mathbf{y}_1^N) &= P(\mathbf{v}_t) P(\tilde{\mathbf{s}}_{t+1}^L) P(\mathbf{y}_1^N | \mathbf{v}_t, \tilde{\mathbf{s}}_{t+1}^L) \\ &= P(\mathbf{v}_t, \mathbf{y}_{1+ct+d_{ct}}^N) P(\tilde{\mathbf{s}}_{t+1}^L, \mathbf{y}_{ct+d_{ct}+1}^N | d_{ct}). \end{aligned}$$

Marginalizing this term over all possible message tails,

$$P(\mathbf{v}_t, \mathbf{y}_1^N) = \sum_{\tilde{\mathbf{s}}_{t+1}^L} P(\mathbf{v}_t, \tilde{\mathbf{s}}_{t+1}^L, \mathbf{y}_1^N)$$

$$= P(\mathbf{v}_t, \mathbf{y}_1^{ct+d_{ct}}) \sum_{\tilde{\mathbf{s}}_{t+1}^L} P(\tilde{\mathbf{s}}_{t+1}^L, \mathbf{y}_{ct+d_{ct}+1}^N | d_{ct}). \quad (3)$$

Both equations (2) and (3) require us to evaluate the probability of receiving a particular sequence. To make the dependence of this quantity on the length of the causal transmitted sequence more explicit, we introduce the following notation.

$$P_M(\mathbf{y}_1^N) = \sum_{\mathbf{x} \in \mathbb{F}_2^M} P(\mathbf{x}, \mathbf{y}_1^N). \quad (4)$$

Applying (3) and (4) in (2), we arrive at the following definition of decoder metric,

$$\begin{aligned} \mu(\mathbf{v}_t) &= \log_2 P(\mathbf{v}_t, \mathbf{y}_1^{ct+d_{ct}}) + \log_2 P_{c(L-t)}(\mathbf{y}_{ct+d_{ct}+1}^N | d_{ct}) \\ &\quad - \log_2 P_{cL}(\mathbf{y}_1^N) \\ &= \log_2 P(\mathbf{s}_0^t) + \log_2 P(\mathbf{d}_0^t) + \log_2 P(\mathbf{y}_1^{ct+d_{ct}} | \mathbf{v}_t) \\ &\quad + \log_2 P_{c(L-t)}(\mathbf{y}_{ct+d_{ct}+1}^N | d_{ct}) - \log_2 P_{cL}(\mathbf{y}_1^N) \\ &= \sum_{i=0}^{t-1} \log_2 P(s_{i+1} | s_i) + P(d_0) \sum_{i=0}^{t-1} \log_2 P(d_{c(i+1)} | d_{ci}) \\ &\quad + \sum_{i=0}^{t-1} \log_2 P(\mathbf{y}_{ci+d_{ci}+1}^{c(i+1)+d_{c(i+1)}} | \mathbf{s}_i^{i+1}, d_{ci}, d_{c(i+1)}) \\ &\quad + \log_2 \frac{P_{c(L-t)}(\mathbf{y}_{ct+d_{ct}+1}^N | d_{ct})}{\log_2 P_{cL}(\mathbf{y}_1^N)}. \end{aligned} \quad (5)$$

The final equality follows from the relative independence of consecutive message blocks and the Markov chain-like behavior of the sequence of drift values.

Since we only consider drift sequences with initial drift $d_0 = 0$, we may set $P(d_0 = 0) = 1$ and thus define equivalent decoder metrics for individual branches of the code tree as

$$\begin{aligned} Z(\mathbf{v}_t \rightarrow \mathbf{v}_{t+1}) &= \mu(\mathbf{v}_{t+1}) - \mu(\mathbf{v}_t) \\ &= \log_2 P(s_{t+1} | s_t) + \log_2 P(d_{c(t+1)} | d_{ct}) \\ &\quad + \log_2 P(\mathbf{y}_{ct+d_{ct}+1}^{c(t+1)+d_{c(t+1)}} | \mathbf{s}_t^{t+1}, d_{ct}, d_{c(t+1)}) \\ &\quad + \log_2 \frac{P_{c(L-t-1)}(\mathbf{y}_{c(t+1)+d_{c(t+1)}+1}^N | d_{c(t+1)})}{P_{c(L-t)}(\mathbf{y}_{ct+d_{ct}+1}^N | d_{ct})}, \end{aligned} \quad (6)$$

where the term $P(\mathbf{y}_{ct+d_{ct}+1}^{c(t+1)+d_{c(t+1)}}, d_{c(t+1)} | \mathbf{s}_t^{t+1}, d_{ct})$ can be computed by an iterative process on a lattice structure, outlined in [12, 15]. A similar method can be used to evaluate the drift likelihood $P(d_{c(t+1)} | d_{ct})$ by setting the horizontal, vertical and diagonal edge weights of the lattice to P_i , P_d and P_t respectively. Alternatively, one may use the closed-form expression specified in [8]. The quantity in (4) can also be evaluated similarly, by assuming that all transmitted sequences $\mathbf{x} \in \mathbb{F}_2^M$ are equally likely. In this case, the corresponding edge weights will simply change to $\frac{P_i}{2}$, P_d and $\frac{P_t}{2}$ respectively.

To obtain an asymptotic expression for (6) as we will require in the next section, the methods from [18–20] are employed.

IV. COMPUTATIONAL ANALYSIS

To assess the complexity of Fano's decoder, it suffices to count the number of forward steps taken by the decoder, since each time a new node is visited, branch metrics for all immediate successors must be computed. This is clearly the most costly step in Fano's algorithm. To establish an upper bound on the total number of visits to nodes in a given code

tree, we adopt the approach and the modeling assumptions outlined in [21], which are summarized in the following.

This analysis is conducted under the assumption of correct decoding. Consider a received vector \mathbf{y}_1^N , which results from the transmission of L blocks, and let the decoding result correspond to the path

$$p^* = ((s_0^*, d_0^*), (s_1^*, d_1^*), \dots (s_L^*, d_L^*)).$$

The remaining nodes that describe all the incorrect paths, are grouped into L subtrees: $\tau_0, \dots, \tau_{L-1}$. Here, τ_i refers to the set of all nodes that hypothesize any false path that stems from \mathbf{v}_i^* , i.e., i^{th} node on the correct path, p^* . If $C'(\mathbf{v}_j)$ refers to the number of visits by decoder to node \mathbf{v}_j , then the total complexity of the complete decoding operation can be expressed as

$$C_{\text{total}} = \sum_{i=0}^{L-1} (C'(\mathbf{v}_i^*) + \sum_{j=i+1}^{L-1} \sum_{\mathbf{v}_j \in \tau_i} C'(\mathbf{v}_j)). \quad (7)$$

We average this quantity over a code ensemble with parameters (c, b) , and all possible transmitted and received sequences. For analytical simplicity, we restrict our attention to codes of infinite memory. Doing so makes the code tree infinite in length, thereby allowing us to assume similar statistical properties for all τ_i . Under this construct, the task of computational analysis may be reduced to the determination of mean decoding complexity per block, which we denote by C_{av} , i.e.,

$$C_{\text{av}} = E[C(\mathbf{v}_0^*)] = E[C(\mathbf{v}_0)] \quad (8)$$

$$\text{where } C(\mathbf{v}_i^*) = C'(\mathbf{v}_i^*) + \sum_{j=i+1}^{L-1} \sum_{\mathbf{v}_j \in \tau_i} C'(\mathbf{v}_j).$$

From the earlier discussion on Fano's algorithm, we can infer that a drop in metric along p^* will cause the decoder to examine alternate paths in the incorrect subtrees. When none of these appear to be promising, the decoder will return to previously visited nodes in p^* , but with a lowered threshold, and can only move forward when the criterion is upheld. Thus, the number of visits to a node clearly depends on its metric.

Let μ_{\min}^* and T_{\min}^* denote the minimum node metric and minimum threshold value along p^* , during a complete decoding operation respectively. It is easy to see that a lower value of T_{\min}^* spurs the decoder to track back more often to explore incorrect nodes in the tree. Hence, one may evaluate C_{av} as

$$\begin{aligned} C_{\text{av}} &= E[C(\mathbf{v}_0^*)] \\ &= \sum_{i=0}^{\infty} P(T_{\min}^* = -i\Delta) E[C(\mathbf{v}_0^*) | T_{\min}^* = -i\Delta]. \end{aligned} \quad (9)$$

The second equality follows from the fact that threshold always starts at 0, and only changes by the magnitude of Δ .

A. Distribution of minimum threshold

We can evaluate the cumulative probability distribution of metric values at depth i along p^* as follows, for any $\sigma < 0$,

$$\begin{aligned} P(\mu_i^* \leq y) &= P(2^{\sigma \mu_i^*} \geq 2^{\sigma y}) \leq 2^{-\sigma y} E[2^{\sigma \mu_i^*}] \\ &= 2^{-\sigma y} E[2^{\sigma \sum_{j=0}^{i-1} Z_j^*}], \end{aligned}$$

where Z_i^* refers to the i^{th} branch metric along p^* . Assuming all Z_i^* 's to be independent and identically distributed yields

$$P(\mu_i^* \leq y) \leq 2^{-\sigma y} (E[2^{\sigma Z^*}])^i = 2^{-\sigma y} (g_0(\sigma))^i. \quad (10)$$

Here $g_0(\sigma)$ is essentially the moment generating function of branch metrics along the correct path. Choosing a suitable

$\sigma_0 < 0$ such that $g_0(\sigma_0) = 1$, we obtain $P(\mu_i^* \leq y) \leq 2^{-\sigma_0 y}$, which implies that

$$P(\mu_{\min}^* \leq y) \leq 2^{-\sigma_0 y}$$

A similar bound may be obtained for T_{\min}^* by exploiting the fact that it can only be 0, or any negative multiple of Δ , i.e.,

$$\begin{aligned} P(T_{\min}^* \leq y) &= P(T_{\min}^* \leq \left\lfloor \frac{y}{\Delta} \right\rfloor \Delta) = P(\mu_{\min}^* \leq \left\lfloor \frac{y}{\Delta} \right\rfloor \Delta + \Delta) \\ &= P(\mu_{\min}^* \leq y + \Delta) \leq 2^{-\sigma_0(y+\Delta)}. \end{aligned} \quad (11)$$

B. Computations in incorrect subtree

To proceed with determining C_{av} , we first recall that the number of visits to any node depends on its metric, and equals the number of unique threshold values with which it is visited. Let the initial and final threshold values with which a node \mathbf{v}_j is visited, be T_1 and T_2 , respectively. They are related by

$$T_1 = T_2 + (C'(\mathbf{v}_j) - 1)\Delta. \quad (12)$$

Additionally from (1) we know that T_1 is related to $\mu(\mathbf{v}_j)$ as

$$T_1 \leq \mu(\mathbf{v}_j) < T_1 + \Delta. \quad (13)$$

Since $T_1 \geq T_{\min}^*$, we can combine (12) and (13) into

$$C'(\mathbf{v}_j) = \left\lfloor \frac{\mu(\mathbf{v}_j) - T_1}{\Delta} \right\rfloor + 1 \leq \frac{\mu(\mathbf{v}_j) - T_{\min}^*}{\Delta} + 1. \quad (14)$$

Using an indicator function $\phi(\mathbf{v}_j)$ defined as

$$\phi(\mathbf{v}_j) = \begin{cases} 1, & \text{if node } \mathbf{v}_j \text{ is visited} \\ 0, & \text{else} \end{cases} \quad (15)$$

the previous inequality may be further refined

$$C'(\mathbf{v}_j) \leq \left(\frac{\mu(\mathbf{v}_j) - T_{\min}^*}{\Delta} + 1 \right) \phi(\mathbf{v}_j) \quad (16)$$

Since the metric of root \mathbf{v}_0^* is always set to zero, we may write

$$\begin{aligned} E[C(\mathbf{v}_0^*)|T_{\min}^* = y] &\leq -\frac{y}{\Delta} + 1 \\ &+ \sum_{j=1}^{\infty} E \left[\sum_{\mathbf{v}_j \in \tau_0^*} C'(\mathbf{v}_j) | T_{\min}^* = y \right]. \end{aligned} \quad (17)$$

To decompose the latter term, we subdivide τ_0 into two subtrees: τ_0' , that contains nodes which hypothesize a wholly inaccurate message sequence, and τ_0^* , which consists of nodes that follow the true message sequence, at least initially, but suggest a different drift sequence.

We now proceed by characterizing the distribution of node metrics, or equivalently branch metrics, in τ_0' . Given their dependence on relative drift changes, these branch metrics are treated in a drift-specific manner. Let $Z'(\delta)$ describe the distribution of branch metrics in τ_0' for a specific drift change δ . Also, let i_{\max} and d_{\max} denote the maximum allowable insertions and deletions over a single block. To bound the number of visits to nodes in τ_0' at depth 1, we proceed as

$$\begin{aligned} E \left[\sum_{\mathbf{v}_1 \in \tau_0'} \left(\frac{\mu(\mathbf{v}_1) - y}{\Delta} + 1 \right) \phi(\mathbf{v}_1) \middle| T_{\min}^* = y \right] \\ = E \left[\sum_{\mathbf{v}_1 \in \tau_0'} \left(\frac{Z(\mathbf{v}_0 \rightarrow \mathbf{v}_1) - y}{\Delta} + 1 \right) \phi(\mathbf{v}_1) \middle| T_{\min}^* = y \right] \\ = (2^b - 1) \sum_{\delta = -d_{\max}}^{i_{\max}} \sum_{z_1 \geq y} \left(\frac{z_1 - y}{\Delta} + 1 \right) P(Z'(\delta) = z_1) \end{aligned}$$

$$= (2^b - 1) \lambda \sum_{z_1 \geq y} \left(\frac{z_1 - y}{\Delta} + 1 \right) P(\zeta' = z_1), \quad (18)$$

where $\lambda = i_{\max} + d_{\max} + 1$ and the variable ζ' uniformly combines the probability distributions of all the drift-specific random variables. By assuming that branch metrics across different levels are independently distributed, we arrive at the following generalization of (18) for higher depths

$$\begin{aligned} E \left[\sum_{\mathbf{v}_j \in \tau_0'} \left(\frac{\mu(\mathbf{v}_j) - y}{\Delta} + 1 \right) \phi(\mathbf{v}_j) \middle| T_{\min}^* = y \right] \\ = (2^b - 1) 2^{b(j-1)} \lambda^j \sum_{\mu \geq y} \left(\frac{\mu - y}{\Delta} + 1 \right) f_j(y, \mu), \end{aligned} \quad (19)$$

where $f_j(y, \mu) = P(\mu'_1 \geq y, \dots, \mu'_{j-1} \geq y, \mu'_j = \mu)$.

In a similar vein, we also analyze the distribution of node metrics in τ_0^* . Evidently, branch metrics in τ_0^* follow a different probability distribution than τ_0' , since the predicted block output is not necessarily independent of the received frame, unlike the previous case. Hence, we let a random variable $Z^*(\delta)$ characterize the distribution of metrics along such branches, for a specific drift change δ . We also note that multiple paths hypothesizing the same message sequence as p^* but with alternate drift sequences, may yield the same node metrics as in p^* . For instance, an all-zero codeword with a nonzero final drift could correspond to multiple drift sequences that seem equally likely. However, for well-behaved codewords, such alternate paths are far more infrequent. Additionally we observe that for higher depths, most of these alternate drift paths lead to a sizeable shift between the received and hypothesized sequences, making them appear random with respect to each other. Thus, we can reasonably assume that all branch metrics in τ_0^* beyond depth 1 can be described by ζ' . By exploiting this assumption and (19), we attempt to bound the number of visits to nodes in τ_0^* .

$$\begin{aligned} \sum_{\mathbf{v}_j \in \tau_0^*} E \left[\left(\frac{\mu(\mathbf{v}_j) - y}{\Delta} + 1 \right) \phi(\mathbf{v}_j) \middle| T_{\min}^* = y \right] \\ = 2^{b'(j-1)} \sum_{\substack{\delta_1^* = -d_{\max} \\ \delta_1^* \neq \delta_1}}^{i_{\max}} P(\delta_1^*) \sum_{z_1 \geq y} P(Z_1^*(\delta_1) = z_1) \sum_{\mu \geq y - z_1} \left(1 + \right. \\ \left. + \frac{\mu - (y - z_1)}{\Delta} \right) f_{j-1}(y - z_1, \mu), \end{aligned} \quad (20)$$

where $b' = b + \log_2 \lambda$. Numerical verification reveals that for reasonable channel parameters, $E[\zeta'] < 0$. This is crucial in ensuring that Fano's decoder is unlikely to pick the wrong successor at any step. It thus follows that any infinite random walk in τ_0 will eventually fall below a finite T_{\min}^* , or

$$\sum_{t=1}^{\infty} \sum_{z < y} f_t(y, z) = 1. \quad (21)$$

Upon further simplification of (19) and (20) using (21), we are able to bound (17) as follows.

$$\begin{aligned} E[C(\mathbf{v}_0^*)|T_{\min}^* = y] &\leq C_1 2^{-\sigma_1 y} + C_2 2^{-(\sigma_0 + \sigma_1) y} \\ &+ C_3 \left(-\frac{y}{\Delta} + 1 \right), \end{aligned} \quad (22)$$

where C_1, C_2 and C_3 are constants for a specific channel and

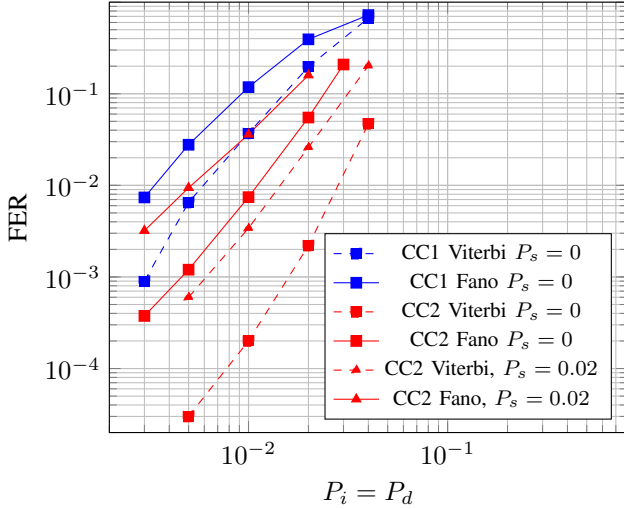


Figure 3. Frame error rate of [3, 1] terminated codes consisting of $L = 100$ information blocks

convolutional code parameters, and $\sigma_1 > 0$ satisfies

$$g_1(\sigma_1) = E[2^{\sigma_1 \zeta'}] = 2^{-b'}. \quad (23)$$

By merging (11) and (22), we obtain a bound for C_{av} , that unfortunately overshoots practical values by several orders of magnitude. However, this bound offers one key insight that C_{av} only converges if

$$\sigma_0 + \sigma_1 < 0. \quad (24)$$

Equation (22) suggests that σ_1 is indicative of the rate of rise of computations in τ_0 . This leads to an intuitive interpretation of (24), that the rate of decline of probability $P(\mu_{\min}^* < y)$, or σ_0 , should sufficiently compensate for the rate of increase of wasteful computations i.e., σ_1 , to allow convergence of average decoding effort per block, i.e., C_{av} . When (24) holds with equality, the channel essentially operates at computational cutoff rate R_0 , which is the code rate beyond which using a sequential decoder becomes computationally impractical. This is due to the fact that for rates exceeding R_0 , the severity of channel noise causes frequent backtracking and more computations in incorrect subtrees. For code trees with infinite depth, C_{av} would be unbounded. On the contrary, for code rates below R_0 , C_{av} is bounded, implying that decoding complexity of a single frame grows linearly with tree depth.

V. RESULTS

To evaluate this decoding strategy, we use two standard, rate 1/3 convolutional codes with distinct constraint lengths, as outlined in Table I.

The generator polynomials are stated in octal form. We simulated the transmission of terminated codewords with

Table I
CONVOLUTIONAL CODES FOR SIMULATIONS

Code	$[c, b, m]$	Gen. polynomial	d_{free}
CC1	[3, 1, 1]	1 3 3	5
CC2	[3, 1, 6]	117 127 155	14

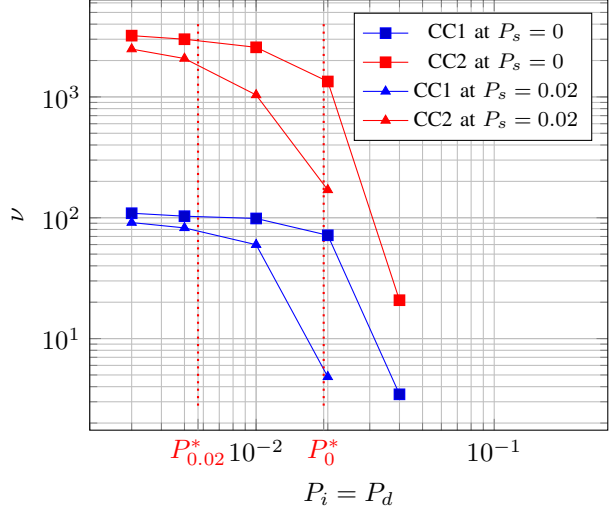


Figure 4. Complexity reduction factor of Fano's decoder for [3, 1] terminated codes consisting of $L = 100$ information blocks

$L = 100$ information blocks, over a channel with parameters set to $P_i = P_d$ and $P_s = 0, 0.02$. To limit decoder complexity, we constrain the maximum allowable insertions/deletions per block to c , and ignore drift states of magnitudes exceeding 30.

A. Decoding performance

The decoding accuracy of Fano's sequential decoder is assessed by measuring frame error rates over a range of $P_i = P_d$, and performing a comparison with Viterbi decoder, as depicted in Fig. 3. Since it only partially examines a given code tree, Fano's decoder is inherently sub-optimal and is thus outperformed by the Viterbi decoder. Unsurprisingly, a higher value of P_s worsens the frame error rate for both decoders.

B. Simulated complexity

The practical complexities of the two decoders are compared in terms of the number of branch metric computations performed. So, for a Viterbi decoder, we compute the total number of branches in the associated trellis, while for Fano's algorithm, it suffices to measure the average number of forward steps taken, denoted by \mathcal{F}_{av} , and to multiply this with the number of outgoing edges per node, as explained in Section IV. For the former case, we limit our attention to the initial non-terminating part of the trellis. Since in either case, a single node produces $2^b(i_{\max} + d_{\max} + 1)$ outgoing branches, we choose to define the following complexity reduction factor,

$$\nu = \frac{\mathcal{N}_{\text{tot}}}{\mathcal{F}_{av}}, \quad (25)$$

where \mathcal{N}_{tot} denotes the total number of nodes in the trellis.

Fig. 4 demonstrates significant reductions in decoding effort by the use of Fano's decoder, particularly for low error probabilities. We also notice that as channel noise deteriorates, especially beyond P_0^* and $P_{0.02}^*$ which mark operation at cutoff rate for substitution probabilities $P_s = 0$ and $P_s = 0.02$ respectively, Fano's decoder gradually loses its computational merit. This is because as error probabilities increase, the decoder is forced to examine many more incorrect paths before the correct one is found.

REFERENCES

- [1] S. M. H. T. Yazdi, H. M. Kiah, E. Garcia-Ruiz, J. Ma, H. Zhao, and O. Milenkovic, "DNA-based storage: Trends and methods," *IEEE Transactions on Molecular, Biological and Multi-Scale Communications*, vol. 1, no. 3, pp. 230–248, Sep. 2015.
- [2] R. Heckel, G. Mikutis, and R. N. Grass, "A characterization of the DNA data storage channel," *Scientific Reports*, vol. 9, no. 9663, Jul. 2019.
- [3] V. I. Levenshtein, "Binary codes capable of correcting deletions, insertions and reversals," *Soviet Physics Doklady*, vol. 10, no. 8, pp. 707–7710, Feb. 1966.
- [4] H. Mercier, V. Bhargava, and V. Tarokh, "A survey of error-correcting codes for channels with symbol synchronization errors," *IEEE Communications Surveys & Tutorials*, vol. 12, no. 1, pp. 87–96, 2010.
- [5] M. C. Davey and D. J. C. MacKay, "Reliable communication over channels with insertions, deletions, and substitutions," *IEEE Transactions on Information Theory*, vol. 47, no. 2, pp. 687–698, Feb. 2001.
- [6] L. Calabi and W. Hartnett, "Some general results of coding theory with applications to the study of codes for the correction of synchronization errors," *Information and Control*, vol. 15, no. 3, pp. 235–249, Sep. 1969.
- [7] D. J. Coumou and G. Sharma, "Insertion, Deletion Codes With Feature-Based Embedding: A New Paradigm for Watermark Synchronization With Applications to Speech Watermarking," *IEEE Transactions on Information Forensics and Security*, vol. 3, no. 2, pp. 153–165, Jun. 2008.
- [8] J. A. Briffa, V. Buttigieg, and S. Wesemeyer, "Time-varying block codes for synchronisation errors: Maximum a posteriori decoder and practical issues," *The Journal of Engineering*, vol. 2014, no. 6, pp. 340–351, Jun. 2014.
- [9] R. G. Gallager, "Sequential decoding for binary channel with noise and synchronization errors," Lincoln Lab Group, Arlington, VA, USA, Tech. Rep., Sep. 1961.
- [10] M. Rahmati and T. M. Duman, "Bounds on the Capacity of Random Insertion and Deletion-Additive Noise Channels," *IEEE Transactions on Information Theory*, vol. 59, no. 9, pp. 5534–5546, Sep. 2013.
- [11] M. F. Mansour and A. H. Tewfik, "Convolutional decoding in the presence of synchronization errors," *IEEE Journal on Selected Areas in Communications*, vol. 28, no. 2, pp. 218–227, Feb. 2010.
- [12] V. Buttigieg and N. Farrugia, "Improved bit error rate performance of convolutional codes with synchronization errors," in *Proc. Int. Conf. Comm.*, London, Jun. 2015, pp. 4077–4082.
- [13] J. M. Wozencraft, "Sequential decoding for reliable communication," Massachusetts Institute of Technology, Tech. Rep., Aug. 1957, p. 182.
- [14] M. F. Mansour and A. H. Tewfik, "Convolutional codes for channels with substitutions, insertions, and deletions," in *Proc. Gobal Commun. Conf.*, vol. 2, Taipei, Taiwan: IEEE, 2002, pp. 1051–1055.
- [15] L. Bahl and F. Jelinek, "Decoding for channels with insertions, deletions, and substitutions with applications to speech recognition," *IEEE Transactions on Information Theory*, vol. 21, no. 4, pp. 404–411, Jul. 1975.
- [16] R. Fano, "A heuristic discussion of probabilistic decoding," *IEEE Transactions on Information Theory*, vol. 9, no. 2, pp. 64–74, Apr. 1963.
- [17] J. Massey, "Variable-length codes and the Fano metric," *IEEE Transactions on Information Theory*, vol. 18, no. 1, pp. 196–198, Jan. 1972.
- [18] R. Pemantle and M. C. Wilson, *Analytic Combinatorics in Several Variables*, ser. Cambridge Studies in Advanced Mathematics 140. Cambridge: Cambridge University Press, 2013.
- [19] S. Melczer and M. C. Wilson, "Asymptotics of lattice walks via analytic combinatorics in several variables," *Discrete Mathematics & Theoretical Computer Science*, vol. DMTCS Proceedings, 28th... P. 6390, Apr. 2020.
- [20] S. Melczer, *An Invitation to Analytic Combinatorics: From One to Several Variables*, ser. Texts & Monographs in Symbolic Computation. Cham: Springer International Publishing, 2021.
- [21] R. Johannesson and K. S. Zigangirov, "Sequential decoding," in *Fundamentals of Convolutional Coding*. Hoboken, New Jersey: John Wiley & Sons, Inc., 2015, pp. 425–484.